Surface Topography Quantification by Integral and Feature-related Parameters

Quantifizieren von Oberflächentopographien mit globalen und objektbezogenen Parametern

U. Wendt*, K. Lange*, M. Smid, R. Ray*** and K.-D. Tönnies******

Using topographical images obtained by confocal laser scanning microscopy, the topography of brittle fracture surfaces and wire-eroded surfaces was quantified. The global topometry values show a significant dependency on the imaging conditions and on the computing algorithm. An algorithm was developed and implemented for the automatic detection and measuring of feature-related parameters in topographies, which uses methods of computational geometry. The software was tested using brittle fracture surfaces of steel.

Key words: algorithm, CLSM, fracture surface, topometry

Die Topographie von Sprödbruchflächen und drahterodierten Oberflächen wurde anhand von Topographiebildern quantifiziert, die mit der konfokalen Laserrastermikroskopie erhalten wurden. Die globalen Parameter besitzen eine deutliche Abhängigkeit von den Abbildungsbedingungen, insbesondere von der Größe und der Form der Voxel, sowie den Algorithmen. Zum objektspezifischen Quantifizieren wurde eine Software auf der Basis von Methoden der algorithmischen Geometrie entwickelt, mit der planare Flächen in Topographien automatisch detektiert und vermessen werden können.

Schlagwörter: Algorithmus, CLSM, Bruchfläche, Topometrie

1 Introduction

Surface topographies contain information about their generation processes and about the influence of crystal structure, microstructure and external loading conditions on those processes. Furthermore, the topography can substantially influence the functionality of structural components. Surfaces generated by fracture, wear, corrosion and machining are of interest, for example.

The quantification of materials topographies can support the establishing and understanding of correlations between processing parameters, microstructure, testing conditions and materials properties and gives hints to the interpretation of the mechanical behaviour. The estimation of only one topometry parameter insufficiently contributes to the quantification of surfaces in some cases [1]. Two types of parameters can be used for surface topography quantification: global parameters and feature-related (object-specific) parameters. The latter describe discrete geometrical objects, for example, planar regions like fracture facets in brittle fracture surfaces. When surface topographies are quantified, it has to be taken into account that the topometry values can depend on the imaging conditions, for instance the optical magnification, and the computing algorithms [2]. This has to be known, if topometry values are used for modelling surface generating processes and if results obtained from several authors are compared.

Two open questions are dealt with in this paper: (i) the influence of measuring conditions and algorithms on the topometry values, and (ii) how features within topography can be detected and measured automatically.

2 Materials and methods

Fracture surfaces of a low-alloyed steel (German brand: 10MnMoNi5-5) and of a white malleable cast iron (EN-GJMW-400-5), and surfaces generated by wire-erosion of a stainless steel (German brand: X6CrNiTi18-11) and of pure copper were studied.

The fracture surfaces (*Figs. 1* and *2*) were obtained by the Charpy impact test of standard V-notched specimens at different temperatures. The eroded surfaces of stainless steel (*Fig. 3*) and copper (*Fig. 4*) were processed by wire-guided electrical discharge machining at a voltage of 85 V, with a discharge time of 1,75 µs, and 2,5 µs, respectively.

The surfaces were imaged by confocal laser scanning microscopy (CLSM) [3], using a beam scanner with an Argon laser (TCS 4D/Leica). With CLSM, the surface topography is optically sectioned, and a topographical image (*Figs. 5* and *6*) is reconstructed from the resulting slice series. The parallel projection of the topographical image (*Fig. 7*) is used for better visualization. All specimens were sputter-coated with Au to get a good and homogeneous reflection of the surface.

The imaging conditions are listed in *Table 1*. An image size of 512 · 512 pixels was chosen for all images. The lateral and

* Otto-von-Guericke-Universität Magdeburg, Fakultät für Maschinenbau, Institut für Werkstofftechnik und Werkstoffprüfung

** Carleton University Ottawa, Ontario/Canada, School of Computer Science

*** Max-Planck-Institut für Informatik Saarbrücken, Algorithms and Complexity Group

**** Otto-von-Guericke-Universität Magdeburg, Fakultät für Informatik, Institut für Simulation und Graphik

Modifizierte Fassung eines Beitrags zum 11. Sommerkurs Werkstofftechnik: Werkstoffentwicklung – Werkstoffanwendung, Magdeburg, 14.–15.6.2002

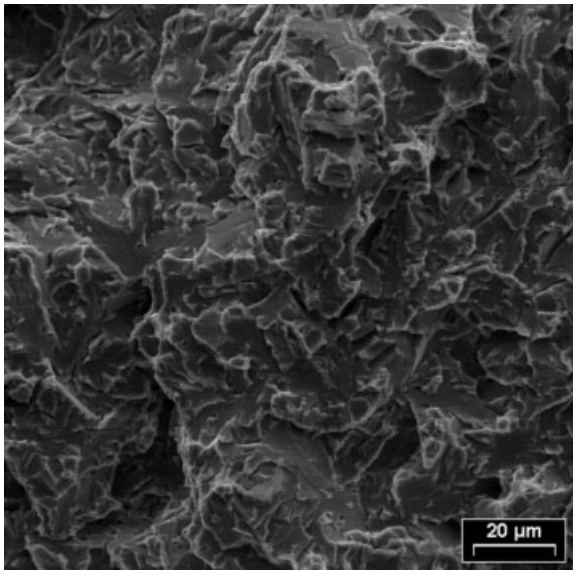

Fig. 1. Fracture surface of the steel 10MnMoNi5-5; testing temperature −120 °C; SEM
Bild 1. Bruchfläche des Stahls 10MnMoNi5-5; Bruchtemperatur − 120 °C; REM

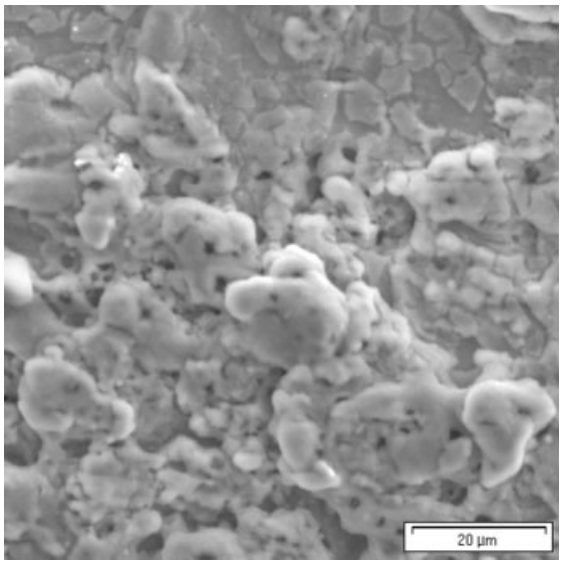

Fig. 3. Eroded surface of the steel X6CrNiTi18-11; SEM
Bild 3. Erodierte Oberfläche des Stahls X6CrNiTi18-11; REM

the axial resolution, obtainable with the used microscope configuration, are 0,3 µm, and 0,7 µm, respectively. The resolution is limited due to the relatively small numerical aperture of objectives with a large working distance (> 1 mm), which is necessary for the investigation of rough surfaces.

In order to avoid the influence of possible textures of the topographies on the topometry values, the fractured specimens were always placed in the same direction on the microscope stage that is with the notch directed to the noon position.

For all image-processing steps and the estimation of the integral parameters, an image analysing system (analysis-pro/ SIS GmbH) was used. A noise filter and the quantification algorithms were implemented using the interpreter language of this image analyser, which is related to the C ++ programming language.

2.1.1 Integral topometry parameters

The normalized surface area (R_S), the mean linear profile segment length (PSL), and the fractal dimension (D) were used as global topometry parameters.

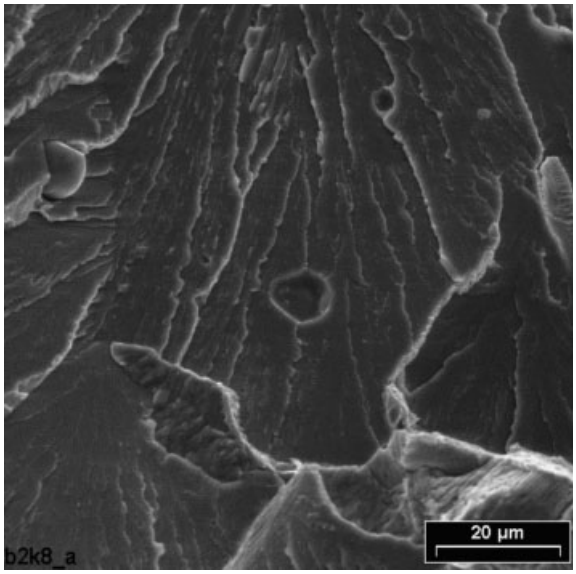

Fig. 2. Fracture surface of white malleable cast iron EN-GJMW-400-5; testing temperature −40 °C; SEM
Bild 2. Bruchfläche von weißem Temperguss EN-GJMW-400-5; Bruchtemperatur −40 °C; REM

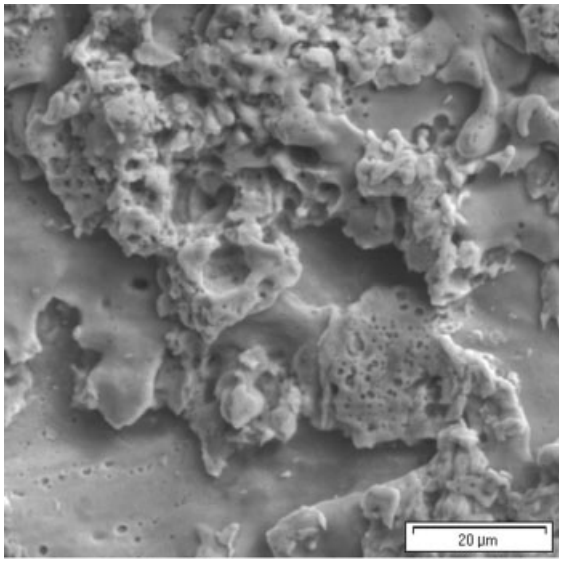

Fig. 4. Eroded surface of copper; SEM
Bild 4. Erodierte Oberfläche von Kupfer; REM

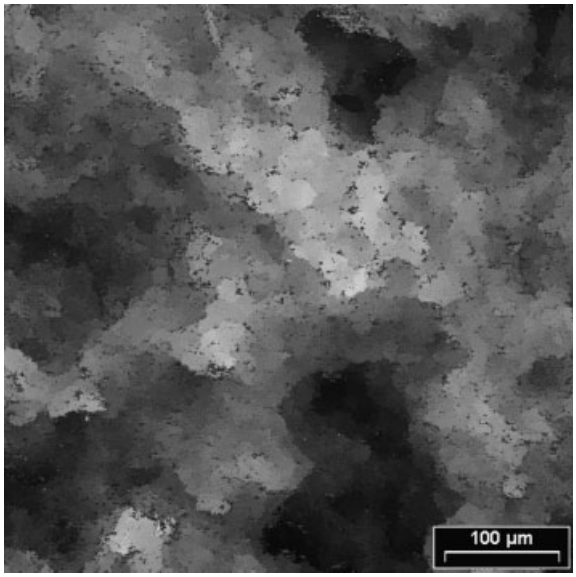

Fig. 5. Fracture surface of the steel 10MnMoNi5-5; testing temperature −120 °C; topographical CLSM image

Bild 5. Bruchfläche des Stahls 10MnMoNi5-5; topographisches CLSM-Bild

The normalized surface area R_S is the ratio of the true surface area A and the projected area A_0: $R_S = A/A_0$.

The true surface area is obtained by triangulation. The area of the triangles was calculated using the Euclidean distance between the voxels. That means, the topography was covered with triangles, and the area of all triangles was summed up to give the true area. The grid size a_{tri} for the triangulation was varied in the range 1 to 6, whereby grid size 1 means that adjacent voxels are used.

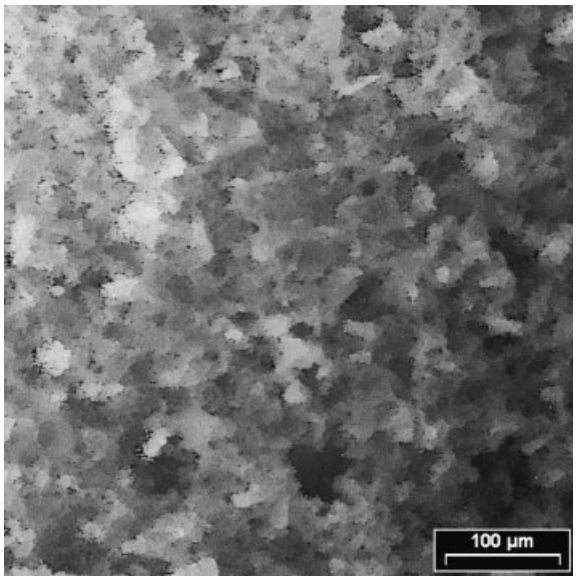

Fig. 6. Eroded surface of the steel X6CrNiTi18-11; topographical CLSM image

Bild 6. Erodierte Oberfläche des Stahls X6CrNiTi18-11; topographisches CLSM-Bild

Fig. 7. Eroded surface of the steel X6CrNiTi18-11; parallel projection of the image in Fig. 6

Bild 7. Erodierte Oberfläche des Stahls X6CrNiTi18-11; Parallelprojektion zu Bild 6

R_S is sensitive to the area of the surface, but not necessarily to its ruggedness. Surfaces with numerous but small peaks can give similar values of R_S as surfaces with only a few but high peaks. For that reason, only surfaces with similar topography features should be compared using R_S.

For the estimation of PSL, height profiles were extracted from the topographical images, and the mean value of the length of the linear segments contained in these profiles was calculated. The Euclidean distance between the endpoints of a linear segment was measured as segment length. A line between two adjacent pixels is also regarded as a linear segment.

For each image, 20 profiles parallel to the x- and to the y-axis were used for the estimation of the mean value. No differences of the mean PSL values of the two directions were detected.

The mean linear profile segment length was chosen as topometry parameter, because it is correlated to certain geometric features contained in topographies, for example, to the size of planar regions in brittle fracture surface topographies.

The fractal dimension is often used for the quantification of topographies, and numerous methods for the estimation of the fractal dimension are known [4, 5, 6]. Here, the slit-island method, the 2d-box-counting method and the triangle method

Table 1. CLSM imaging parameters

Tabelle 1. Parameter bei der CLSM-Bildaufnahme

Objective magnification/ numerical aperature	**Scan area** [µm · µm]	**Side length of cubic voxels** [µm]
5×/0,12	2000 × 2000	3,91
10×/0,25	1000 × 1000	1,95
20×/0,45	500 × 500	0,98
40×/0,6	250 × 250	0,49
100×/0,75	100 × 100	0,195

were chosen. These methods are based on relatively simple algorithms and work properly on all investigated specimens.

For the slit-island method [7], height slices were performed on topographical images with different grey value thresholds, leading to islands and lakes in the topographical image. The area and the perimeter of these islands and lakes were measured, and a log-log plot was drawn. The fractal dimension is calculated from the slope of the curve as $D_{si} = 2/\text{slope}$.

The 2d-box-counting method [8] uses height profiles, extracted from the topographical image and drawn as x-y-curves in the image analyser, which are masked with grids of different box sizes (e). The number of hits (n; boxes covering at least one pixel) is counted, and the fractal dimension is calculated from the slope of the log-log plot of n vs. e, as $D_{2dbox} = \text{slope}$.

The triangle method is based on a triangulation of the surface using different triangle sizes (a_{tri}). The fractal dimension is calculated from the slope of the R_S-a_{tri} plot as D = 2-slope. This method is comparable to the yardstick (ruler, divider) method, which is often applied to profiles or object perimeters [9].

2.1.2 Feature-related topometry parameters

Fracture facets in brittle fracture surfaces were used as an example for feature specific topometry. They are regarded simplifying as „more or less planar regions“, because they show a certain roughness and sometimes a little sweeping. The detection criterion was that the facets possess a minimum projection size of eight pixels. From each planar region, the coordinates, the true area and the normal were calculated.

3 Results

3.1 Software for feature-related quantification

The aim of the developed algorithm is to solve the problem of computing the largest regions in a terrain which are approximately planar heuristically in an acceptable time, which depends on the number of objects n of the image: $\mathbf{O}(n^2 \log n (\log \log n)^3)$. The principle of the algorithm is that the surface is triangulated and the normal of every triangle is calculated. Normals with a pre-selected deviation (for example 10 degrees) are then checked, if the triangles are neighbours that is if they share an edge. The algorithm has already been described in detail elsewhere [10].

The algorithm is implemented as a programme we called „PlaneFinder“, which can be run on local computers and on a remote server using the World Wide Web. It is written in C ++ and uses the LEDA library [11]. The results are stored as a data sheet in a data processing file format. Several

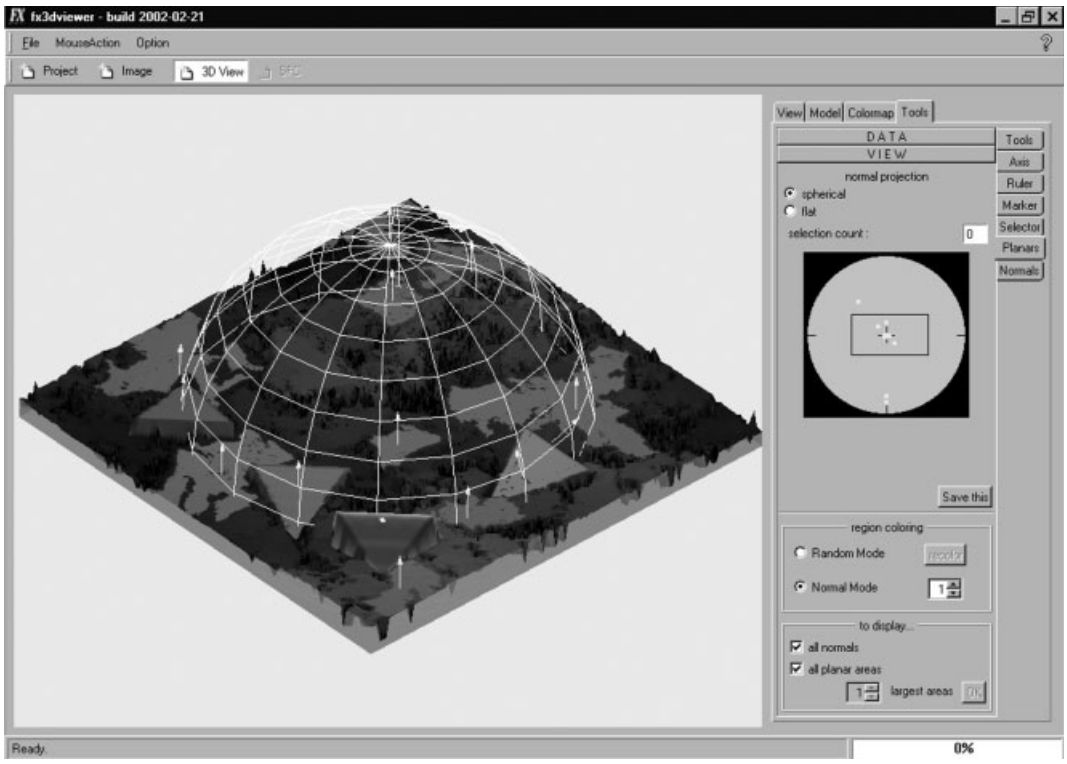

Fig. 8. Screenshot of the visualization software fx3dviewer showing topometry results obtained by the PlaneFinder software. The illustration shows as well original planar regions (fracture facets) as artificial triangles with their normals to demonstrate the performance of the software. Brittle fracture surface of the steel 10MnMoNi5-5. The sphere is drawn to improve the 3D-view

Bild 8. Screenshot der Benutzeroberfläche fx3dviewer zur Visualisierung der durch die Software PlaneFinder erhaltenen Topometrieergebnisse. Die Abbildung zeigt sowohl reale planare Flächen (Bruchfacetten) als auch künstlich eingefügte Dreiecke mit ihren Normalen, um die Arbeitsweise der Software zu verdeutlichen. Sprödbruchfläche des Stahls 10MnMoNi5-5. Das Kugelgitter ist zur Verbesserung des räumlichen Eindrucks eingezeichnet

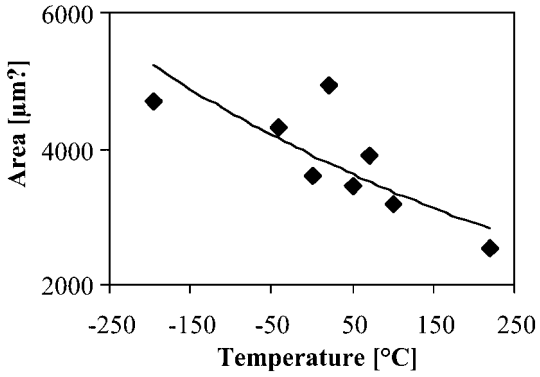

Fig. 9. Mean area of the 20 largest fracture facets vs. testing temperature; detection and measurement of the areas by PlaneFinder; white malleable cast iron; impact test

Bild 9. Mittlere Fläche der 20 größten Bruchfacetten in Abhängigkeit von der Prüftemperatur; Detektion und Berechnung der Flächen mittels PlaneFinder; weißer Temperguss; Kerbschlagbiegeversuch

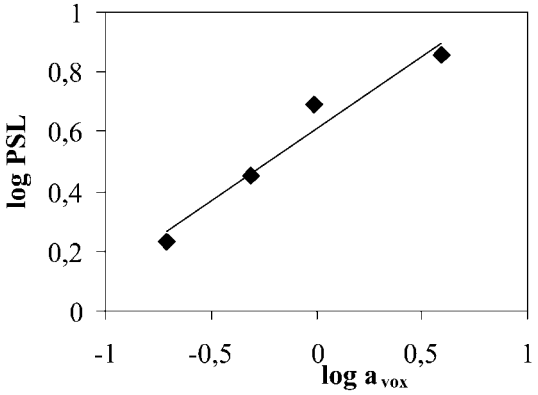

Fig. 10. Dependency of the PSL on the voxel size a_{vox}; eroded surface of the stainless steel

Bild 10. Abhängigkeit der Profilsegmentlänge von der Voxelgröße; erodierte Oberfläche des Stahls X6CrNiTi18-11

data are calculated for each planar region: coordinates of the region within the image, true area, and normal direction.

To visualize the computed results, a platform called „fx3dviewer“ was developed, which can be used with any computer system. The detected planar regions and their normals can be shown in parallel-projection images (*Fig. 8*).

Additionally, the interface contains some tools for interactive measurements on topographical images.

The planar areas, which have been detected and measured by PlaneFinder, are used for correlations with fracture conditions.

An example of the application of the topometry results is the relationship between the mean area of the 20 largest fracture facets, which are regarded as planar regions, and the specimen temperature during the impact test (*Fig. 9*). With increasing testing temperature, the fracture facets become smaller, due to the locally increased deformability of the material.

3.2 Influence of imaging conditions and algorithm on topometry data

To study the dependency of the PSL-values on the voxel size, PSL was measured using topographical images received with different magnifications and which therefore have different cubic voxel sizes. This relationship between PSL and voxel size has to be taken into account, if PSL is used for the numerical modelling of crack paths.

Furthermore, the same region of the surface was imaged with different numbers of optical slices, so that tetragonal voxels with different z scaling are resulting.

The obtained PSL-values depend on the voxel size as demonstrated for the eroded surface of the stainless steel (*Fig. 10*). The curve is a straight line. From the slope of the curve, a kind of fractal dimension for profiles can be calculated as $D_{PSL} = 1 + \text{slope}$. *Fig. 10* shows results obtained for cubic voxels. If the shape of the voxels becomes tetragonal with different z scaling, a non-linear curve results (*Fig. 11*).

With small z scaling, the PSL increases with growing step size, but it becomes constant at a step size greater than 0,8 µm. This value corresponds to the axial resolution of the microscope of 0,77 µm for the used objective. Obviously, the influ-

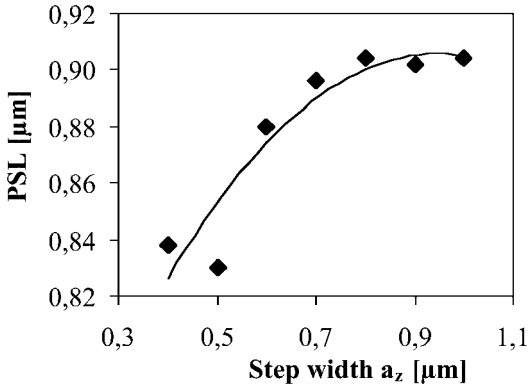

Fig. 11. Relationship between the voxel shape and the PSL; eroded surface of the stainless steel; x, y-scaling = 0,2 µm

Bild 11. Zusammenhang zwischen der Voxelform und der Profilsegmentlänge; erodierte Oberfläche des rostfreien Stahls; x,y-Skalierung der Voxel = 0,2 µm

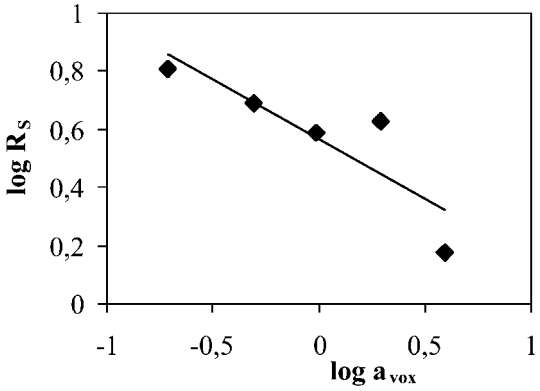

Fig. 12. Log-lot plot of normalized surface area R_S vs. the size of cubic voxels a_{vox}; wire eroded surface of the steel X6CrNiTi18-11; triangle size = 1 voxel

Bild 12. Abhängigkeit der normierten Oberfläche von der kubischen Voxelgröße; erodierte Oberfläche des Stahls X6CrNiTi18-11; Abmessungen der Triangulationsdreiecke = 1 Voxel

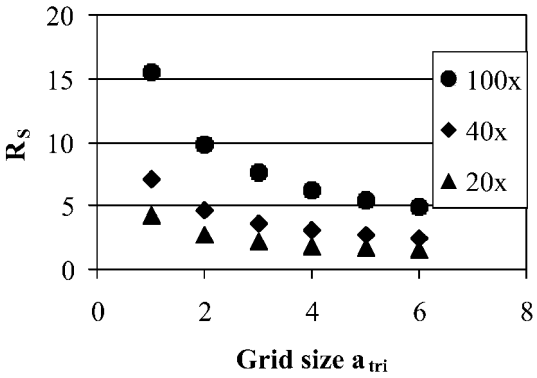

Fig. 13. Influence of the triangulation grid size a_{tri} on the normalized surface area R_S for different voxel size (given is the optical magnification of the used objectives); wire-eroded surface of copper

Bild 13. Einfluss der Maschengröße bei der Triangulation auf die normierte Oberfläche bei unterschiedlichen Voxelgrößen (angegeben ist die Vergrößerung der Objektive); erodierte Oberfläche von Kupfer

ence of the voxel shape on the measured value disappears with step size values greater than the axial resolution.

The eroded specimens were used to study the influence of the voxel size on the normalized surface R_S. Cubic voxels with different sizes were obtained with different optical magnifications and related z step sizes.

The log-log plot of R_S vs. voxel size (*Fig. 12*) gives an almost straight line for the eroded surface of the stainless steel. The fractal dimension can be obtained from the slope of the curve as $D_{RSvox} = 2\text{-slope}$. The explanation for the curve is that with different voxel sizes topographical features with different sizes are included in the measurement. More of the fine details of the topography are imaged with higher magnification, and they contribute to the measurement, if the voxel size is equal or larger than the optical resolution.

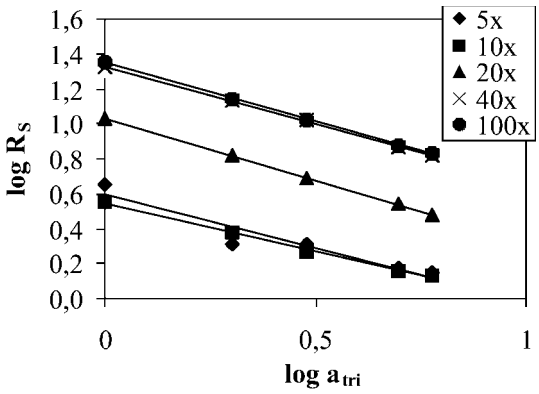

Fig. 14. Log-log-plot of normalized surface area R_S vs. the size of the grid a_{tri} for the triangulation; fracture surface of the steel 10MnMoNi5-5; cubic voxel sizes (given is the magnification of the objectives)

Bild 14. Abhängigkeit der normierten Oberfläche von der Maschengröße bei der Triangulation; Bruchfläche des Stahls 10MnMoNi5-5; kubische Voxel (gegeben ist die Vergrößerung der Objektive)

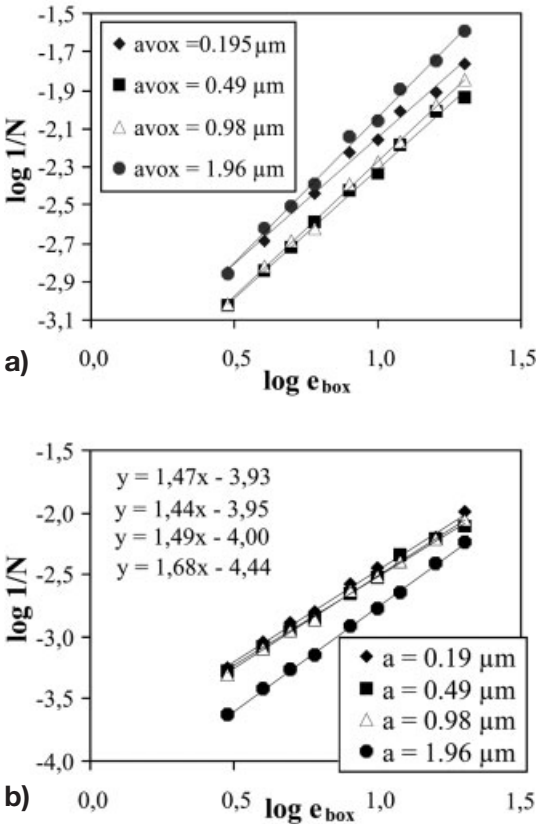

Fig. 15. Estimation of the fractal dimension by box-counting performed on profiles, which are extracted from topographical images with different voxel sizes a_{vox}; a) fracture surface of the low-alloyed steel; b) eroded surface of the stainless steel

Bild 15. Ermittlung der fraktalen Dimension mittels der Box-Counting-Methode, angewandt auf Höhenprofile; Ausgangspunkt sind topographische Aufnahmen mit unterschiedlicher Voxelgröße; a) Bruchfläche des Stahls 10 MnMoNi5-5; b) erodierte Oberfläche des Stahls X6CrNiTi18-11

R_S not only depends on the imaging conditions (here the size and the shape of the voxels) but also on the size of the triangles a_{tri} used for triangulation (*Fig. 13*). R_S decreases with increasing grid size. This decrease itself depends on the voxel size (that is the optical magnification).

Straight lines are also resulting in the log R_S vs. log a_{tri} plot for the brittle fracture surface of the low-alloyed steel (*Fig. 14*).

With the box-counting method for the estimation of the fractal dimension, straight lines result for images with the same voxel size, but different curves are obtained for different voxel sizes (*Figs. 15a* and *15b*).

The slit-island method was performed by slicing the topography at several grey levels. For the fracture surface of the low-alloyed steel as well as for the eroded surface of the stainless steel, it could be shown that for grey value thresholds at 20, 50 and 80% of the maximal grey value in the image, the log-log plots of the area vs. the perimeter of the lakes and islands result in separate curves for each threshold (*Figs. 16a* and *16b*).

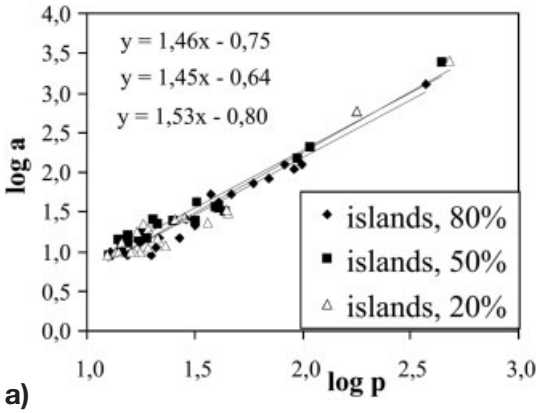

a)

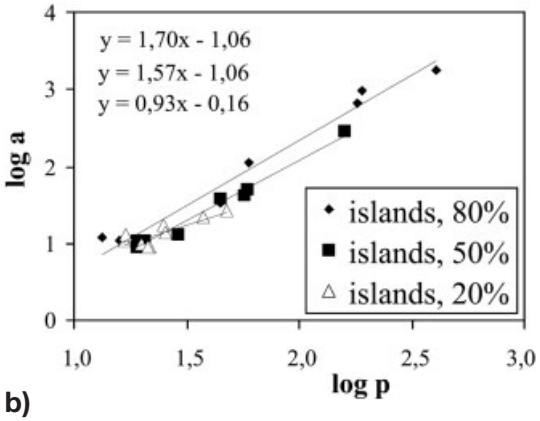

b)

Fig. 16. Slit-island method for the estimation of the fractal dimension; plot of the area (a) and perimeter (p) of the islands; a) for the fracture surface of the steel 10MnMoNi5-5, b) for the eroded surface of the steel X6CrNiTi18-11

Bild 16. Slit-Island-Methode zur Ermittlung der fraktalen Dimension; aufgetragen sind Fläche und Umfang der Inseln; a) Bruchfläche des Stahls 10MnMoNi5-5; b) erodierte Oberfläche des Stahls X6CrNiTi18-11

4 Conclusions

An algorithm for the automatic detection of planar regions in surface topographies was developed and implemented as a software called PlaneFinder. The software uses topographical images, which are obtained by confocal laser scanning microscopy. Furthermore, the software is applicable to all topographical images, obtained by other methods, by which surfaces can be imaged three-dimensionally: scanning force microscopy, scanning electron microscopy combined with stereophotogrammetry, reconstruction of 3D-images from conventional optical slices (extended focus imaging), and white light interferometry.

For the visualization of the results, the software fx3dviewer was developed. The topometry results obtained by the PlaneFinder programme are used to establish correlations between the topography, the materials microstructure, and fracture conditions.

The global parameters used to quantify surface topographies are influenced by the imaging conditions, especially the size and the shape of the voxels, and the algorithm. This has to be taken into account, if topometry values reported by different authors are compared. In all cases, the imaging method (voxel size) and the algorithm have to be taken into consideration.

5 References

1. *Wendt, U., Blumenauer, H.,* Materialprüfung, *41* (1999) 190–193: Konfokale Laserrastermikroskopie – Mehr Informationen aus Bruchflächen gewinnen.
2. *Wendt, U., Lange, K., Smid, M.,* J. Microsc., accepted 7/2002: Influence of imaging conditions and computing algorithms on the quantification of surface topography.
3. *Wilson, T.,* Confocal Microscopy, Academic Press, London 1992.
4. *Lea Cox, B., Wang, J.S.Y.,* Fractals, *1* (1993) 87–115: Fractal Surfaces: Measurement and Applications in the Earth Sciences.
5. *Wendt, U., Kaestner, M.,* Cell Vision – J. Anal. Morphol., *4* (1997) 179–180: Fractal analysis of steel and ceramic fracture surfaces using CLSM and AFM images.
6. *Tricot, C., Ferland, P., Baran, G.,* wear, *172* (1994) 127–136: Fractal analysis of worn surfaces.
7. *Charkaluk, E., Bigerelle, M., Iost A.,* Engin. Fract. Mech., *61* (1998) 119–139: Fractals and fracture.
8. *Dubuc, B., Quiniou, J.F., Roques-Carmes, C., Tricot, C., Zucker; S.W.,* Phys. Rev., A *39* (1989) 1500–1512: Evaluating the fractal dimension of profiles.
9. *Lung, C.W., March, N.H.,* Mechanical Properties of Metals, World Scientific, Singapore, 1999.
10. *Smid, M., Ray, R., Wendt, U., Lange, K.,* Discrete Applied Mathematics, accepted 7/2002: Computing Large Planar Regions in Terrains, with an Application to Fracture Surfaces.
11. *Mehlhorn, K., Näher, S.,* Communications of the ACM, *38* (1995) 96–102: LEDA, a platform for combinatorial and geometric computing.

This work was supported by the Deutsche Forschungsgemeinschaft, grants WE 2301/3-2 and SM 57/4-1. The authors thank Mathias Gumz, Jan Tusch, Ulrike Landfried and Boyan Ivanov, all students at the Otto von Guericke University Magdeburg, for the design and the implementation of the software, and for microscopical imaging.

Anschrift: Herrn Prof. Dr.rer.nat. habil. *U. Wendt*, Institut für Werkstofftechnik u. Werkstoffprüfung, Fakultät für Maschinenbau, Universität Magdeburg, Postfach 41 20, 39016 Magdeburg

Received in final form: 7/22/02 [T 523]